BIOPHARMACEUTICS & DRUG DISPOSITION
Biopharm. Drug Dispos. **36**: 462–480 (2015)
Published online 11 June 2015 in Wiley Online Library
(wileyonlinelibrary.com) **DOI**: 10.1002/bdd.1959

Verapamil hepatic clearance in four preclinical rat models: towards activity-based scaling

J. Nicolaï[a], T. De Bruyn[a], P. P. Van Veldhoven[b], J. Keemink[a], P. Augustijns[a], and P. Annaert[a,*]
[a]*Drug Delivery and Disposition, KU Leuven Department of Pharmaceutical and Pharmacological Sciences, O&N2, Leuven, Belgium*
[b]*Laboratory of Lipid Biochemistry and Protein Interactions, KU Leuven Department of Cellular and Molecular Medicine, O&N1, Leuven, Belgium*

ABSTRACT: The current study was designed to cross-validate rat liver microsomes (RLM), suspended rat hepatocytes (SRH) and the isolated perfused rat liver (IPRL) model against *in vivo* pharmacokinetic data, using verapamil as a model drug. Michaelis-Menten constants (K_m), for the metabolic disappearance kinetics of verapamil in RLM and SRH (freshly isolated and cryopreserved), were determined and corrected for non-specific binding. The 'unbound' K_m determined with RLM (2.8 μM) was divided by the 'unbound' K_m determined with fresh and cryopreserved SRH (3.9 μM and 2.1 μM, respectively) to calculate the ratio of intracellular to extracellular unbound concentration ($Kp_{u,u}$). $Kp_{u,u}$ was significantly different between freshly isolated (0.71) and cryopreserved (1.31) SRH, but intracellular capacity for verapamil metabolism was maintained after cryopreservation (200 vs. 191 μl/min/million cells). Direct comparison of intrinsic clearance values (Cl_{int}) in RLM versus SRH, yielded an activity-based scaling factor (SF) of 0.28–0.30 mg microsomal protein/million cells (MPPMC). Merging the IPRL-derived Cl_{int} with the MPPMC and SRH data, resulted in scaling factors for MPPGL (80 and 43 mg microsomal protein/g liver) and HPGL (269 and 153 million cells/g liver), respectively. Likewise, the hepatic blood flow (61 ml/min/kg b.wt) was calculated using IPRL Cl_{int} and the *in vivo Cl*. The scaling factors determined here are consistent with previously reported CYP450-content based scaling factors. Overall, the results show that integrated interpretation of data obtained with multiple preclinical tools (i.e. RLM, SRH, IPRL) can contribute to more reliable estimates for scaling factors and ultimately to improved *in vivo* clearance predictions based on *in vitro* experimentation. Copyright © 2015 John Wiley & Sons, Ltd.

Key words: scaling factors; hepatic clearance; verapamil; suspended hepatocytes; isolated perfused liver; liver microsomes; $Kp_{u,u}$

Introduction

Liver microsomes (LM) used to be the preferred *in vitro* system to predict metabolic clearance [1]. However, with the current isolation and cryopreservation techniques, suspended hepatocytes have become an equally accepted tool to evaluate metabolic stability [2]. First of all, hepatocytes still possess a plasma membrane and transmembrane drug transporters, both controlling intracellular drug exposure. Secondly, hepatocytes contain the complete arsenal of phase II metabolic enzymes including UDP-glucuronosyltransferase, monoamine oxidase and aldehyde oxidase, which are absent or not evaluated in liver microsomes [3]. Hepatocyte suspensions thus constitute a more universally applicable clearance prediction tool. In addition, in the past two decades, a lot of effort has been invested in unraveling the relationship

*Correspondence to: Drug Delivery and Disposition, KU Leuven Department of Pharmaceutical and Pharmacological Sciences, O&N2, Herestraat 49, Box 921, B-3000 Leuven, Belgium.
E-mail: pieter.annaert@pharm.kuleuven.be

Received 11 September 2014
Revised 9 January 2015
Accepted 20 April 2015

between intrinsic clearance (Cl_{int}) values estimated with either liver microsomes or hepatocytes [4–7]. The rate limiting step, be it passive permeability, active transport or metabolism, determines whether a good correlation between these model systems is obtained [2,8]. This illustrates that a direct comparison of *Cl* estimates obtained in different models for hepatic drug disposition is instrumental for better mechanistic understanding of the actual *in vivo* situation. In addition, correcting *in vitro* Cl_{int} values for the unbound fraction (fu) to liver microsomes and hepatocytes, although far from trivial [10–12], clearly results in significantly improved predictions [9]. However, in suspended hepatocytes as well as *in vivo*, intracellular unbound concentrations ($C_{u,intracellular}$), accessible for metabolic enzymes, will rarely equal the extracellular unbound concentrations due to transporter activity, intracellular binding, sequestration processes and/or pH partitioning [10,11]. This holds true especially for compounds showing poor permeation across the hepatocellular plasma membrane (e.g. ionized and/or polar compounds). Consistently, intracellular concentrations of substrates for active uptake transporters (OATP1B1/3, OATP2B1, OAT2, OCT1) and/or efflux transporters (MRP2/3/4/6, P-gp, BSEP, BCRP) will be significantly higher or lower than free extracellular concentrations [12–14]. Consequently, unless only CYP-mediated metabolism is involved for a freely diffusing compound, direct comparison between Cl_{int} values determined with rat liver microsomes and suspended rat hepatocytes are hampered by the absence of a plasma membrane and plasma-membrane associated proteins in rat liver microsomes. Indeed, the Cl_{int} measured with suspended hepatocytes will have to be corrected for $C_{u,intracellular}$ to obtain an (hepatocyte-based) unbound intracellular intrinsic clearance ($Cl_{int,hep,intracellular}$), which can be compared with the unbound Cl_{int} obtained with microsomes ($Cl_{int,mic,u}$). The required $C_{u,intracellular}$ can be calculated by multiplying $C_{u,extracellular}$ with the ratio of intracellular to extracellular concentration, also known as $Kp_{u,u}$. Recently, this parameter was determined either by methods based on imaging (e.g. Raman, PET) or by approaches implying tissue homogenization [10,15,16].

The initial aim of this work was to cross-validate rat liver microsomes with suspended rat hepatocytes by evaluating *in vitro* Cl_{int} predictions in these model systems against measurements in the isolated perfused rat liver (IPRL) and *in vivo*. Verapamil, which is subject to hepatic elimination through metabolism, was used as the model compound. Verapamil consists of a racemic mixture of (R)- and (S)-verapamil. It is used as an L-type Ca^{2+}-channel blocker for treating hypertension, angina and atrial dysrhythmias [17]. It is subject to extensive hepatic metabolism in humans (i.e. *O*- and *N*-dealkylation) via CYP3A4, 1A2 and 2C9 [18]. Similarly in rats, this dealkylation is primarily orchestrated by Cyp3a1/2 and 1a2, resulting in a hepatic extraction ratio for verapamil of 80%–90% [19]. Although being a potent inhibitor of P-gp, the biliary clearance of verapamil is overshadowed by metabolism and passive transmembrane permeation [20]. This well-defined disposition profile makes verapamil a suitable 'first candidate' to compare data obtained in rat liver microsomes, suspended rat hepatocytes and IPRL with *in vivo* data that were all generated in the present study.

Comparison of the obtained elimination kinetics between microsomes and hepatocytes provided a novel promising approach to calculate $Kp_{u,u}$. This parameter was subsequently applied to calculate an activity-based scaling factor (SF) for microsomal protein per million cells (MPPMC). Additional comparison with data obtained in the isolated perfused rat liver (IPRL) yielded a scaling factor for microsomal protein per gram liver (MPPGL) and hepatocytes per gram liver (HPGL). Likewise, combining *in vivo* and *ex vivo* values in the well-stirred model, resulted in an experimentally determined hepatic blood flow rate ($Q_{H,B}$), closely matching the reported $Q_{H,B}$ values. Finally, a two-compartmental model was applied to predict retrospectively the *in vivo* pharmacokinetic profile of verapamil with the obtained *in vitro* and *ex vivo* data.

Materials and Methods

Materials

(R,S)-Verapamil.HCl, VERA; butyl 4-hydroxybenzoate; 1-aminobenzotriazole, ABT; 4-morpholinepropanesulfonic acid, MOPS; (ethylenedinitrilo) tetraacetic acid, EDTA; sucrose; sodium phosphate (monobasic, di-basic); glucose 6-phosphate, G6P;

ethylene-bis(oxyethylenenitrilo)tetraacetic acid, EGTA; collagenase type IV (*C. histolyticum*, ≥ 125 CDU); Percoll®; Leibovitz-15, L-15 powder (with glutamine); triethylamine, TEA; taurocholic acid sodium salt hydrate, TCA and sodium hydroxide were all purchased from Sigma-Aldrich (Schnelldorf, Germany). Trypan blue stain (0.4%); L-glutamine (200 mM; penicillin–streptomycin mixture (contains 10000 IU potassium penicillin and 10000 IU streptomycin sulfate per ml in 0.85% saline), 10X phosphate buffered saline, PBS and fetal bovine serum, FBS were obtained from Lonza SPRL (Verviers, Belgium). Dimethylsulfoxide, DMSO and methanol, MeOH were purchased from Acros Organics (Geel, Belgium). Glycerol (anhydrous); $MgCl_2.6H_2O$; acetonitrile, ACN; Na-acetate and acetic acid were purchased from Analar-Normapur (VWR) (Leicestershire, England). Na_4-NADPH was obtained from Merck Millipore (MA, USA). $CaCl_2$ and $NaHCO_3$ were obtained from Chem-lab NV (Zedelgem, Belgium) and NaCl from Fisher Chemical (Landsmeer, Netherlands). Dulbecco's modified Eagle medium, DMEM and William's E medium, WEM were purchased from Life Technologies (Paisley, UK) and HEPES (4-(2-hydroxyethyl)-1-piperazineethanesulfonic acid) from MP Biochemical (Illkirch, France).

Animals

Male Wistar rats were purchased from Janvier (Le Genest Saint Isle, France) and were housed according to Belgian and European laws, guidelines and policies for animal experiments, housing and care in the Central Animal Facility of the KU Leuven. All experiments involving laboratory animals were approved by The Institutional Ethical Committee for Animal Experimentation (license number: .LA1210261).

Determination of unbound fractions

The fu_{mic}, fu_{hep}, fu_{IPRL} and fu_{plasma} were all determined by equilibrium dialysis performed with a HTDialysis apparatus (CT, USA) using membranes with a molecular mass cut-off of 12–14 kDa. The HTDialysis apparatus was subjected to circular agitation (175 rpm) at 37 °C and samples were taken from both sides in each well at 4 h and 6 h. Each dialysis experiment was conducted in triplicate at a verapamil concentration of 10 μM (0.2% v/v DMSO). The fu_{hep} was determined with freshly isolated and cryopreserved hepatocytes (pool of three batches), metabolically inactivated by heat (50 °C, 15 min) or pre- and co-incubation with 1-aminobenzotriazole (1 mM, 30 min). The integrity and viability of heat-inactivated cells was determined using the Trypan blue (0.04%) exclusion method. The compositions of the dialysis media are shown in the supplemental data (supplemental Table 1).

Preparation of rat liver microsomes

Three male Wistar rats (197–200 g) were fasted for a period of 24 h, prior to preparation of rat liver microsomes. Following anesthesia (120 mg/kg of ketamine + 24 mg/kg xylazine i.p.), the liver was perfused with homogenization buffer (5 mM MOPS, 1 mM EDTA, 250 mM sucrose, sparged with 95% O_2/5% CO_2, pH 7.4, 4 °C) until all blood was removed. Immediately after initiating the perfusion, the animals were killed by severing the diaphragm. After all blood had been removed, the liver was excised, minced with surgical scissors and added to ice cold homogenization buffer (3 ml/g tissue). The tissue mixture was homogenized in a glass/Teflon potter homogenizer with 15 up and down strokes (15 s/stroke, 1200 rpm) while keeping it on ice. After repeating this step for three livers, the liver homogenates were pooled. The pooled tissue homogenate was sampled for the determination of P450 content and centrifuged ($4000 \times g$) for 10 min at 4 °C. After suspending the pellet with homogenization buffer and repeating the centrifugation step, the supernatants were combined and transferred to polycarbonate ultracentrifuge tubes (Fisher Scientific, Landsmeer, The Netherlands). The pooled supernatants were centrifuged ($15000 \times g$) for 20 min at 4 °C, after which the pellet was discarded and the supernatant was ultra-centrifuged ($150000 \times g$) for 70 min at 4 °C. The resulting microsomal pellet was washed with homogenization buffer and ultracentrifugation was repeated ($150000 \times g$) for 35 min at 4 °C. The microsomal pellet was homogenized in microsomal storage buffer (5 mM MOPS, 1 mM EDTA, 20% w/v glycerol) with a glass/Teflon potter homogenizer (2–3 up and down strokes, 800 rpm). A sample of the microsomes was taken for total microsomal

DOI: 10.1002/bdd

protein determination and aliquots (500 µl) were stored at −80 °C.

Determination of total microsomal protein and P450 content

The total microsomal protein was determined with the BCA protein assay kit (Pierce Chemical, Rockford, IL, USA). Total P450 content was determined for both liver homogenates and liver microsomes with the method of Omura and Sato [21]. The microsomal protein concentration was 16.84 mg/ml and the total P450 content was 0.73 nmol/mg protein. The MPPGL was calculated to be 44.5 mg/g liver and the yield of this method amounted to 51% of the total hepatic P450 content.

Incubations with rat liver microsomes

Rat liver microsomes stored at −80 °C were thawed and kept on ice. Subsequently they were diluted with microsomal incubation buffer (MIB) (3 mM $MgCl_2$, 100 mM sodium phosphate buffer pH 7.4) to acquire a four-fold concentrated rat liver microsome protein solution. Verapamil was diluted in MIB to acquire a two-fold concentrated solution (0.4% DMSO). Incubations were performed in 48-well plates (Greiner-Bio-One, Wemmel, Belgium) on a shaking incubator (350 rpm, 37 °C). Verapamil (200 µl) was preincubated with rat liver microsomes (100 µl) for 5 min. Incubations were initiated by adding a freshly prepared prewarmed (37 °C) NADPH solution (1 mM final concentration) containing G6P (3 mM final concentration), resulting in an incubation volume of 400 µl [22]. Samples (75 µl) were taken at different time points and were added to an equal volume of ice-cold acetonitrile (ACN) to quench the enzymatic activity. Samples were stored at −20 °C for at least 1 h prior to analysis. Immediately before analysis, the samples were thawed and centrifuged (10500 × *g*) for 10 min at 21 °C, the supernatants were transferred into micro-inserts for HPLC analysis. Linearity studies were performed with respect to the verapamil concentration, microsomal protein concentration and incubation time. Subsequently, optimal conditions for determining the *in vitro* half-life were selected (i.e. different microsomal protein concentrations were selected for different incubation concentrations of verapamil, supplemental Table 2). All incubations were terminated after 10 min and performed in triplicate ($n = 3$) for each concentration. The experiment was performed in duplicate with the rat liver microsome pool. Michaelis-Menten parameters for the metabolic disappearance of verapamil by rat liver microsomes were determined by non-linear regression analysis in R (version i386 2.15.3).

Isolation of rat hepatocytes

Hepatocytes were isolated from male Wistar rats (180–210 g) using a modified version of the collagenase perfusion method described previously [23]. The rat was anesthetized (120 mg/kg ketamine + 24 mg/kg xylazine i.p.). The liver was cannulated (16-gauge cannula) via the portal vein and the thoracic vena cava inferior and perfused with Ca^{2+}-free buffer (118.1 mM NaCl, 25 mM $NaHCO_3$, 5.5 mM glucose, 1 mM EGTA, 4.7 mM KCl, 1.2 mM KH_2PO_4, sparged with 95% O_2/5% CO_2, pH 7.4, 37 °C) in a recirculating manner. The abdominal vena cava inferior was tied with a suture to ensure unidirectional flow. After 10 min, 50 mg of collagenase type IV (*C. histolyticum*, ≥ 125 CDU) was added to 50 ml of the recirculating Ca^{++}-free buffer and 1 ml of $CaCl_2$ (0.5 M) was added within 1 min. The liver was perfused with the collagenase containing buffer until it was visibly digested (5–8 min), removed from the rat and washed once with ice-cold basal cell culture medium (BCM) (William's E medium, 5% v/v FBS, 2 mM glutamine, 100 U/ml penicillin, 100 µg/ml streptomycin). The Glisson's capsule was torn gently to release the hepatocytes into fresh BCM. The resulting hepatocyte suspension was filtered through a 100 µm nylon filter, the volume was adjusted to 50 ml with BCM and centrifuged (50 × *g*) for 3 min at 4 °C. The hepatocyte pellet was gently resuspended in BCM and the volume was adjusted to 40 ml. The hepatocytes were counted three times in a hemocytometer and the viability was determined using the Trypan blue (0.04%) exclusion method. Viability was always ≥ 85% and the yield was $9–13 \times 10^6$ cells/ml. An aliquot of the hepatocyte suspension was centrifuged (50 × *g*) for 3 min at 4 °C and the pellet was resuspended in adjusted L-15 medium

(L-15*, supplemental data). The hepatocytes were counted three times in a hemocytometer and the viability was determined using the Trypan blue (0.04%) exclusion method. The suspension was diluted to the desired cell densities and kept at 4 °C until the start of the experiment.

Freezing and thawing of suspended rat hepatocytes

An aliquot of freshly isolated hepatocyte suspension in BCM was centrifuged ($50 \times g$) for 3 min at 4 °C and the pellet was resuspended in ice-cold cryoprotective medium (Synth-a-Freeze®, Gibco, Gent, Belgium) to result in a cell density of 10^6 cells/ml. The cells were frozen with a freezing cycle containing a supercooling phase. After reaching −100 °C, the cells were stored in liquid nitrogen. Immediately before the experiments, the hepatocytes were thawed by gently shaking the vials in a water bath (37 °C). After all the ice had melted, the suspension was transferred to the thawing solution (37 °C) consisting of 25 ml thawing medium (DMEM, 4 mM glutamine, 1 µM dexamethasone, 4 µg/ml insulin, 100 U/ml penicillin, 100 µg/ml streptomycin) and 16 ml Percoll® (90% Percoll®, 10% 10X PBS). The suspension volume was adjusted to 50 ml with thawing medium (37 °C) and centrifuged ($168 \times g$) for 20 min at 21 °C. The resulting pellet was gently resuspended in 20 ml of thawing medium (37 °C) and centrifuged ($50 \times g$) for 3 min at 21 °C. The resulting pellet was resuspended in the desired incubation medium (37 °C). The hepatocytes were counted three times in a hemocytometer and the viability was determined using the Trypan blue (0.04%) exclusion method. The viability was always > 70%. The cells were diluted to the desired cell densities and kept on ice until the start of experiments.

Incubations with suspended rat hepatocytes

Freshly isolated or cryopreserved suspended rat hepatocytes in L-15* were two-fold concentrated and 300 µl of the hepatocyte suspension was preincubated for 10 min in 24-well plates (Greiner-Bio-One, Wemmel, Belgium) on a shaking incubator (37 °C, 300 rpm). Incubations were initiated by adding 300 µl of two-fold concentrated verapamil in L-15* (0.4% DMSO). This medium ensured that cryopreserved and freshly isolated suspended rat hepatocytes performed equally well for verapamil metabolism (supplemental Table 2) and incubations could be performed at atmospheric CO_2 without change of the pH. All reactions were quenched by adding aliquots to two volumes of ice-cold MeOH. These samples were stored at −20 °C for the duration of at least 1 h prior to analysis. Just before analysis, the samples were thawed and centrifuged ($20816 \times g$) for 10 min at 21 °C, the supernatants were transferred into micro-inserts for HPLC analysis. Linearity studies were performed with respect to verapamil concentration, hepatocyte concentration and incubation time. Subsequently, optimal conditions for determining the *in vitro* half-life were selected (i.e. different hepatocyte densities were selected for different incubation concentrations of verapamil, supplemental data). Samples were taken at 0, 10, 20 and 30 min and all incubations were performed in triplicate ($n = 3$) for each concentration of verapamil with three different batches/pools of freshly isolated/cryopreserved hepatocytes. Michaelis-Menten parameters for the metabolic disappearance of verapamil by freshly isolated and cryopreserved suspended rat hepatocytes ($n = 3$) were determined by non-linear regression analysis in R (version i386 2.15.3).

Isolated perfused rat liver

Male Wistar rats (285–325 g) were anesthetized and the portal vein was cannulated according to the rat hepatocyte isolation procedure. The thoracic vena cava inferior was severed without cannulation and the abdominal vena cava inferior was closed with a surgical clip. The bile duct was cannulated with 10–15 cm of PE-10 tubing (0.28 mm × 0.61 mm i.d. × o.d.). To maintain bile flow, taurocholic acid was infused continuously into the circulating system (30 µmol/h). During excision, the liver was perfused (30 ml/min) with sparged (95%/5% O_2/CO_2) Krebs-Henseleit buffer (KHB). Following hepatectomy, the liver was placed on a collecting platform in a humidified and temperature controlled (37 °C) chamber. Perfusion with KHB was continued until 30 min after cannulation. After organ acclimatization, the perfusion system was switched to KHB + 20% rat blood (flow rate = 21.4 ± 3.3 ml/min), containing 1.6 µmol of verapamil to reach an initial perfusate concentration of 20 µM, which was

DOI: 10.1002/bdd

oxygenated by sparging with carbogen (95%/5% O_2/CO_2) through a fritted metal bulb. The perfusate was sampled (100 µl) just before and after the liver at 2 min intervals until 10 min and every 5 min until 25 min after dosing. Bile samples were collected every 5 min. After a 5 min wash-out period, the next dose of verapamil (16 µl, 100 mM) was added to the perfusate reservoir (this was repeated three times). Liver functionality was monitored by measuring bile flow, portal vein pressure and visual appearance. Perfusate and bile samples were stored at −20 °C until analysis. A blank perfusion (= without liver) was performed to assess adsorption to the perfusion set-up. Tubing materials consisted of THV, Tygon® chemical and Teflon®.

In vivo study

Male Wistar rats (360–420 g) were allowed free access to food and water for the duration of the study. Rats were put in a temperature-regulated cage (37 °C) 10 min before taking any blood sample. Rats were dosed with 5 mg/kg of verapamil (5 mg/ml in 0.9% NaCl) i.v. via the lateral tail vein as a single bolus, administered over 10 s. Blood samples were collected from the opposite side of the tail before verapamil administration and at 5, 10, 20, 30, 60, 120, 180, 240 and 300 min after dosing. Each blood sample, consisting of 200–300 µl of blood, was collected in a heparinized tube and kept on ice until sample preparation. Blood samples were precipitated in 2 volumes of acetonitrile containing the internal standard (butyl 4-hydroxybenzoate, 37.5 µM), vortexed (2 × 30 s) and stored at −20 °C until analysis.

Determination of blood:plasma (B:P) partitioning

To determine the B:P ratio, the rats were treated the same way as described for the *in vivo* study, but samples were taken only at 30, 60 and 180 min after dosing. Samples consisted of 500–600 µl of blood and an aliquot of each sample was centrifuged (2880 × *g*) for 15 min at 37 °C. The pellet was discarded and the upper plasma layer was treated in the same way as for a blood sample. Concentrations in whole blood were divided by concentrations in plasma to determine the B:P ratio.

Bioanalysis

The HPLC system consisted of a Waters 600 multisolvent delivery system with controller and column oven (30 °C), Waters 717 plus autosampler with temperature control (21 °C), a Waters 2475 fluorescence detector (ex/em: 230/312 nm) and a Gemini® C18 column (3 µm, 4.6 mm × 150 mm, Phenomenex, Utrecht, The Netherlands). The mobile phase consisted of 60:40 v/v% buffer:MeOH under isocratic conditions. The buffer used was a 25 mM sodium acetate buffer containing 10 mM triethylamine (pH 5.5). The flow rate was kept at 0.6 ml/min, the retention time of verapamil was 7.8 min, the run time was 10 min. Quality control samples (QCs) of 10 µM and 2 µM were prepared and stored under the same conditions as the samples. For suspended rat hepatocyte QCs, interday repeatability RSDs and accuracy amounted to 4.5% and 102.5% ($n = 6$) for 10 µM and 5.7% and 111.5% ($n = 6$) for 2 µM, respectively. For rat liver microsomes QCs, interday variability and accuracy amounted to 2.5% and 100.3% ($n = 5$) for 10 µM, and 5.0% and 94.4% ($n = 5$) for 2 µM.

On the day of analysis, isolated perfused rat liver samples were thawed and proteins were precipitated with two volumes of acetonitrile containing internal standard (butyl 4-hydroxybenzoate, 37.5 µM) and vortexed (2 × 30 s). From this point IPRL and *in vivo* samples were processed in the same manner. Next, the samples were centrifuged (20816 × *g*) for 10 min at 4 °C. The supernatants were transferred into clean glass test tubes and evaporated to dryness under a gentle stream of air. The residue was dissolved into one volume of mobile phase (51% buffer, 39% MeOH, 10% acetonitrile). The buffer of the mobile phase for the analysis of the IPRL and *in vivo* samples consisted of 25 mM sodium acetate containing 10 mM triethylamine (pH 5.8). The samples were vortexed, transferred into microcentrifuge tubes and centrifuged again (20816 × *g*) for 10 min at 21 °C. The supernatants were transferred into micro-inserts for HPLC-vials and injected directly into the HPLC-system. Fluorescence detection was performed using two different conditions (ex/em), namely 230/312 nm and 268/347 nm for verapamil and butyl 4-hydroxybenzoate, respectively. The flow rate was 0.6 ml/min under isocratic conditions for 16 min and was followed

DOI: 10.1002/bdd

by a wash-step (80:20 ACN:H_2O) for 2 min. The retention times were 11 min and 14 min for verapamil and butyl 4-hydroxybenzoate, respectively. The interday variability and accuracy for blood sample QCs amounted to 8.6% and 99.5%, 7.0% and 99.2% and 8.5% and 101.2% or 10 μM, 1 μM and 0.1 μM, respectively. The interday variability and accuracy for IPRL sample QCs amounted to 2.2% and 99.3%, 5.4% and 101.1% and 9.6% and 109.8% for 10 μM, 1 μM and 0.1 μM, respectively. The observed peaks were integrated using Empower Pro (Empower 2) software and data analysis was performed with Microsoft Excel 2010.

Data analysis and statistics

The slope of verapamil disappearance (Ln(C)) was used to determine the *in vitro* half-life of verapamil metabolism [9]. This half-life was used to calculate the velocity of metabolism by either rat liver microsomes or suspended rat hepatocytes at every concentration (pmol/min/mg microsomal protein or pmol/min/million cells) (Eq. (1)).

$$v = \left(\frac{0.693}{t_{1/2}} \times \frac{\mu l \text{ well volume}}{\text{million cells } \textbf{\textit{or}} \text{ mg protein}} \right) \times [verapamil] \quad (1)$$

Using R software (version i386 2.15.3) Michaelis-Menten curves were fitted to data pooled from multiple experiments and V_{max} and K_m (± SE) were determined. An *F*-test ($\alpha = 0.05$) was performed to assess the difference between fits for the individual and pooled data sets. No significant difference was observed and pooled fits were used for further calculations. A two-tailed Student's *t*-test was used to evaluate statistical differences between parameter values (GraphPad Prism 5 for Windows; GraphPad Software Inc., San Diego, CA) at an α level of 0.05. Subsequently, intrinsic clearance values (Cl_{int}) were calculated according to Equation (2).

$$Cl_{int} = \frac{V_{max}}{K_m} \quad (2)$$

Cl_{int} has to be corrected for binding of compound to different sources of protein (e.g. microsomes, hepatocytes) by using Equation (3), since only the unbound drug is subjected to metabolism [9]. In this way, $Cl_{int,hep,u}$ and $Cl_{int,mic,u}$ can be calculated.

$$Cl_{int,u} = \frac{Cl_{int}}{fu} = \frac{V_{max}}{K_m \times fu} \quad (3)$$

Michaelis-Menten constants for verapamil metabolism by hepatocytes were obtained with extracellular verapamil concentrations. Since metabolic enzymes reside in the intracellular compartment, these K_m values only represent an apparent K_m (Figure 1). Thus, the metabolic unbound K_m as measured with hepatocytes ($Km_{hep,u}$) represents the unbound extracellular K_m ($Km_{hep,u,ex}$) according to Equation (4).

$$Km_{hep} \times fu_{hep} = Km_{hep,u,ex} \quad (4)$$

When using rat liver microsomes, P450-mediated metabolism is measured without restrictions regarding membrane permeability. As these enzymes are expected to retain their affinity (i.e. K_m) towards specific compounds, multiplying the metabolic K_m as measured with rat liver microsomes (Km_{mic}) and fu_{mic}, yields a value for the intracellular unbound enzymatic K_m or Km_{enzyme} (Eq. (5)). The latter assumption is also applied in current PBPK-modeling settings [24].

$$Km_{mic} \times fu_{mic} = Km_{mic,u} = Km_{enzyme} \quad (5)$$

As a consequence, the K_m ratio of Km_{enzyme} over $Km_{hep,u,ex}$ gives a direct measure of the ratio of an intracellular unbound concentration to an extracellular unbound concentration (Eq. (6)). This factor, which could be lower than, equal to, or higher than 1 (Figure 1) is known as $Kp_{u,u}$ [15].

$$\frac{Km_{enzyme}}{Km_{hep,u,ex}} = Kp_{u,u} \quad (6)$$

When $Kp_{u,u}$ is multiplied by the unbound extracellular K_m (Eq. (4)), the unbound intracellular K_m can be calculated and Cl_{int}/fu from Equation (3) can be written as shown in Equation (7).

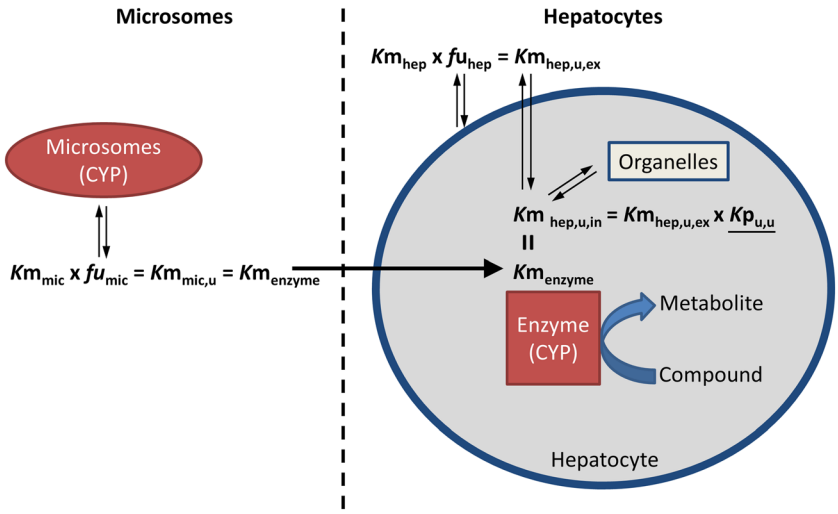

Figure 1. Scheme illustrating the relationship between the intracellular unbound K_m ($Km_{hep,u,in}$) and extracellular unbound K_m ($Km_{hep,u,ex}$). When Km_{mic} is multiplied with fu_{mic}, $Km_{mic,u}$ is obtained, which (as shown on the left side) corresponds to the enzymatic K_m or Km_{enzyme}. As shown on the right side, Km_{enzyme} equals the unbound metabolic K_m inside the hepatocyte or $Km_{hep,u,in}$. $Km_{hep,u,in}$ is related to the extracellular unbound K_m or $Km_{hep,u,ex}$, which can be calculated by multiplying Km_{hep} with fu_{hep}. This relation between $Km_{hep,u,in}$ and $Km_{hep,u,ex}$ can be described by $Kp_{u,u}$, representing the ratio of unbound intracellular to unbound extracellular concentration. This $Kp_{u,u}$ can be calculated by dividing $Km_{hep,u,in}$ by $Km_{hep,u,ex}$

$$Cl_{\text{int,hep,intracellular}} = \frac{Vmax_{\text{hep}}}{Km_{\text{hep}} \times fu_{\text{hep}} \times Kp_{\text{u,u}}} \quad (7)$$

Theoretically, the intracellular unbound clearance within hepatocytes should equal the unbound microsomal clearance, which is calculated with Equation (3). Since unbound concentrations are being considered, the rat liver microsomes and suspended rat hepatocytes can be 'matched' based on activity [25]. In this way, an activity-based scaling factor between rat liver microsomes and suspended rat hepatocytes, such as microsomal protein per million cells (MPPMC), can be calculated according to Equation (8).

$$MPPMC = \frac{Cl_{\text{int,hep,intracellular}}}{Cl_{\text{int,mic,u}}} = \frac{\left(\frac{Vmax_{\text{hep}}}{Km_{\text{hep,u}} \times Kp_{\text{u,u}}}\right)}{\left(\frac{Vmax_{\text{mic}}}{Km_{\text{mic,u}}}\right)} = \frac{\left(\frac{Vmax_{\text{hep}}}{Km_{\text{hep,u}} \times \frac{Km_{\text{mic,u}}}{Km_{\text{hep,u}}}}\right)}{\left(\frac{Vmax_{\text{mic}}}{Km_{\text{mic,u}}}\right)} = \frac{Vmax_{\text{hep}}}{Vmax_{\text{mic}}} \quad (8)$$

Because IPRL-perfusate samples were taken before and after the liver, an extraction ratio for the IPRL experiments (ER_{IPRL}) was calculated according to Equation (9), which can be used to calculate Cl_{IPRL} according to Equation (10). However, this calculation did not yield a single Cl_{IPRL} value, since ER_{IPRL} was variable with time due to the distribution process as well as to the mechanism-based inhibition of metabolism [26]. Therefore, this calculation was regarded inaccurate and was not used for further calculations.

$$ER_{\text{IPRL}} = 1 - \frac{C_{\text{out}}}{C_{\text{in}}} \quad (9)$$

$$Cl_{\text{IPRL}} = Q_{\text{IPRL}} \times ER_{\text{IPRL}} \quad (10)$$

Since the perfusate concentration–time profile during IPRL experiments showed a pronounced distribution phase, a two-compartmental model (Eq. (11)) was used to determine Cl_{IPRL} by dividing the dose by the AUC [27].

$$Cp = A \times e^{-\alpha t} + B \times e^{-\beta t} \quad (11)$$

Theoretically, Cl_{IPRL} values could then be used to estimate intrinsic Cl_{IPRL} with the well-stirred model. However, the required assumptions associated with the well-stirred model were not met

DOI: 10.1002/bdd

in our IPRL set-up since instant and homogeneous distribution of drug inside the liver did not occur and unbound concentrations in the perfusate did not equal the unbound concentrations in the liver [28]. Thus, *C*p0, k_{el}, V_d and $Cl_{int,IPRL}$ were calculated based on outflow concentrations, as those can be assumed to reflect equilibrium with liver tissue, once the distribution phase is over. *C*p0 was calculated by extrapolating the elimination slope of the outflow concentrations to t_0. In this way, *C*p0 reflects the concentration assuming immediate distribution of the administered dose. V_d is calculated by dividing the administered dose by *C*p0 and this V_d is finally multiplied by k_{el} to acquire $Cl_{int,IPRL}$. $Cl_{int,IPRL}$ is subsequently scaled to *in vivo* with a scaling factor regarding g liver/kg b.wt (determined for each individual IPRL experiment). To correct the calculated clearance for binding to the perfusate, $Cl_{int,IPRL}$ was divided by fu_{IPRL} to obtain the unbound $Cl_{int,IPRL}$ or $Cl_{int,IPRL,u}$. $Cl_{int,IPRL,u}$ was determined for the first two doses of verapamil and the mean $Cl_{int,IPRL,u}$ per liver was calculated. The mean values were combined to obtain a mean (± SD) value for all livers ($n = 3$). Since the metabolic activity towards verapamil between suspended rat hepatocytes and isolated perfused rat liver can be matched, the acquired $Cl_{int,IPRL,u}$ values can be used to determine the scaling factor regarding hepatocytes/g liver and microsomal protein/million cells according to Equations (12) and (13).

$$HPGL = \frac{Cl_{int,IPRL,u}}{Cl_{int,hep,u}} \tag{12}$$

$$MPPGL = MPPMC \times HPGL \tag{13}$$

To predict the organ clearance ($Cl_{int,organ,u}$) based on $Cl_{int,u}$ for suspended rat hepatocytes, scaling by HPGL can be applied. The verapamil fraction unbound in blood (fu_B) was then combined with $Cl_{int,organ,u}$ in the well-stirred model ($Q_{H,B} = 70$ ml/min/kg b.wt) to calculate $Cl_{in\ vivo}$ (Eq. (14) and (15)) [28–30]. Calculations were also performed using the parallel tube and dispersion models (supplemental Table 5) [31]. However, no significant difference was observed compared with the results obtained with the well-stirred model. Therefore the simplest model (i.e. well-stirred model) was applied.

$$fu_B = fu_{Plasma} \times \left(\frac{Cp}{Cb}\right) \tag{14}$$

$$Cl_{in\ vivo} = \frac{Q_{H,B} \times fu_B \times Cl_{int,organ,u}}{Q_{H,B} + fu_B \times Cl_{int,organ,u}} \tag{15}$$

In vivo PK parameters, with PK data from the *in vivo* study, were calculated by assuming a two-compartmental model as described above for IPRL (Eq. (11)). *In vivo* clearance was used to estimate the *in vivo* intrinsic hepatic clearance ($Cl_{int,organ,u}$) with the transformed well-stirred model (Eq. (16)). Herein, the value of $Q_{H,B}$ (i.e. 55.2 ml/min/kg b.wt or 70 ml/min/kg b.wt) is key in determining the outcome of all clearance predictions [30,32,33]. Therefore, $Q_{H,B}$ was determined (Eq. (17)) based on *in vivo* and *ex vivo Cl* values obtained here and this value was compared with the literature values. This activity-based hepatic blood flow ($Q_{H,B}$) can be calculated since $Cl_{int,organ,u}$ matches $Cl_{int,IPRL,u}$ and $Cl_{in\ vivo}$ is known from *in vivo* studies.

$$Cl_{int,organ,u} = \frac{\frac{1}{fu_B}}{\frac{1}{Cl_{in\ vivo}} - \frac{1}{Q_{H,B}}} \tag{16}$$

$$Q_{H,B} = \frac{1}{\frac{1}{Cl_{in\ vivo}} - \frac{1}{fu_B \times Cl_{int,organ,u}}} \tag{17}$$

In vivo predictions

To evaluate their accuracy, *in vitro/ex vivo* data were used to predict the *in vivo* PK profile. For this purpose, Equation (19) was transformed into Equation (20) so that β becomes dependent on the predicted *in vivo* clearance (*Cl*) while *A*, *B*, *Dose* and γ were kept constant. We chose to retain γ as a constant, since α is dependent on β (Eq. (18)). Thus, the 'distribution slope' (α) will also be affected by the 'elimination slope' (β).

$$\gamma = \alpha - \beta \tag{18}$$

DOI: 10.1002/bdd

$$AUC = \frac{Dose}{Cl} = \frac{A}{\gamma + \beta} + \frac{B}{\beta} \quad (19)$$

$$Dose \times \beta^2 + (\gamma \times Dose - B \times Cl - Cl \times A) \times \beta + B \times \gamma \times Cl = 0 \quad (20)$$

Since $Cl_{int,mic,u}$ values represent an 'intracellular' unbound Cl, we have to correct for a possibly altered distribution of the compound in the presence of the plasma membrane. Therefore, $Cl_{int,mic,u}$ had to be multiplied by the average $Kp_{u,u}$ to acquire a corrected (i.e. 'extracellular') $Cl_{int,mic,u}$ which can be used in the well-stirred model to calculate the *in vivo* Cl_{int} [34]. All predicted Cl_{int} values were recalculated with the well-stirred model to produce *in vivo* clearance values. These values were recalculated from ml/min/kg b.wt to l/h with the experimentally determined average body weight (0.38 ± 0.03 kg). The resulting Cl was used in Equation (20) to calculate β.

Results

Determination of unbound fractions

Unbound fractions of verapamil in the presence of different sources of protein (i.e. plasma, blood, KHB + 20% blood, suspended rat hepatocytes, rat liver microsomes) were determined. The results are shown in Table 1. The unbound fractions of verapamil in the presence of hepatocytes inactivated by heat or 1-aminobenzotriazole did not differ, thus the mean values of both experiments are shown. However, a statistically significant difference was found between the unbound fractions of verapamil with either freshly isolated (0.86 ± 0.08) or cryopreserved hepatocytes (0.78 ± 0.04) ($p < 0.0001$). The medium-loss approach showed that the total incubate-to cell concentration ratio was a constant (= fu_{hep}) for different concentrations of verapamil, at different cell densities (data not shown). The latter justifies the use of a single fu_{hep} value for further calculations.

Table 1. Experimentally determined values for blood to plasma (B:P) ratio as well as unbound fraction (fu) of verapamil in the presence of different protein sources. Values are means ± SD (n = at least 3)

Parameter	Value ± SD	Parameter	Value ± SD
fu_{mic}	0.68 ± 0.02	fu_{plasma}	0.26 ± 0.02
$fu_{hep,fresh}$	0.86 ± 0.08	fu_{IPRL}	0.50 ± 0.04
$fu_{hep,cryo}$	0.78 ± 0.04	*B:P*	0.81 ± 0.05

In vivo study

Male Wistar rats (360–420 g) were dosed with 5 mg/kg verapamil (5 mg/ml in 0.9% saline). Blood samples were collected before verapamil administration and at 5, 10, 20, 30, 60, 120, 180, 240 and 300 min after dosing (Figure 2). Blood concentration–time profiles were analysed following a two-compartmental model: $t_{1/2}$ (0.86 ± 0.06 h), Vd_{ss} (1.34 ± 0.1 L) and Cl (53.4 ± 7 ml/min/kg b.wt) (Table 2). Using the well-stirred model ($Q_{H,B}$ = 70 ml/min/kg b.wt [30]), the *in vivo* clearance was converted to the *in vivo* $Cl_{int,organ}$ value (693 ml/min/kg b.wt). Since verapamil is primarily eliminated by the liver, this reflects the hepatic Cl_{int}.

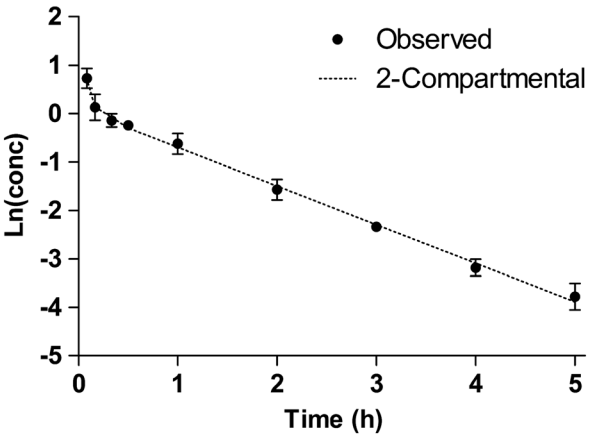

Figure 2. Ln(blood concentration, mg/l)-time curve of verapamil in Wistar rats (360–420 g, n = 3) dosed i.v. with 5 mg/kg of verapamil. Points represent mean values ± SD. The dotted line represents the *in vivo* PK-profile based on two-compartmental parameters calculated from observed data. PK-parameters were calculated assuming a two-compartmental model and are shown in Table 2

Isolated perfused rat liver

IPRL experiments were performed to compare the *in vitro* clearance data of verapamil, determined with suspended rat hepatocytes and rat liver microsomes, with the actual hepatic clearance values and the *in vivo* data. The perfusate concentration–time profiles are shown in Figure 3. The recovery of

Table 2. *Ex vivo* and *in vivo* pharmacokinetic parameters of verapamil in the Wistar rat. *In vivo Cl* was recalculated to a Cl_{int} value according to the well-stirred model ($Q_{H,B}$ = 70 ml/min/kg b.wt) [30]. IPRL Cl was scaled to kg b.wt with an experimentally determined scaling factor of 35 g liver/kg b.wt. Values are means ± SD (n = at least 3)

PK parameter	*In vivo* (5 mg/kg)	IPRL (20 μM)
$t_{1/2}$ (h)	0.86 ± 0.06	0.14 ± 0.03
Vd_{ss} (l)	1.34 ± 0.1	2.28 ± 0.5
Cl (ml/min/kg b.wt)	53 ± 7	667 ± 74
Cl_{int} (ml/min/kg b.wt)	693 (419–1381)	1335 ± 183

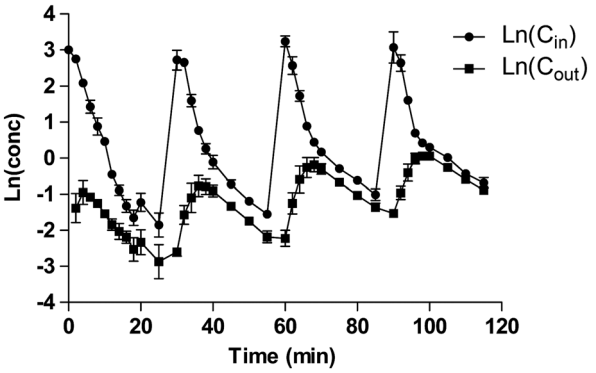

Figure 3. Ln(perfusate concentration, μM)-time profiles of verapamil during isolated perfused rat liver experiments. Ln (C_{in}) and Ln(C_{out}) represent perfusate concentrations immediately before and after the liver, respectively. Points are mean values ± SEM of three separate IPRL experiments (dose: 1.6 μmol, flow rate: 18–24 ml/min)

verapamil in a perfusion-experiment without liver was 97%, thus non-specific binding to the perfusion-system was regarded as negligible. Post-hepatic concentrations (C_{out}) reached a maximum following each dose as shown in Figure 3, illustrating the distributional equilibrium between perfusate and organ at the end of a distribution phase and the beginning of the elimination phase. The ER_{IPRL} was calculated according to Equation (9) and is shown in Figure 4. It clearly shows the change of ER_{IPRL} with time and consequentially the inability to use ER_{IPRL} to calculate Cl_{IPRL}. Therefore, as described in the data-analysis section, outflow concentrations were used to determine Cp0, or the initial perfusate concentration assuming immediate distribution of the administered dose. Subsequently, $t_{1/2}$ (0.14 ± 0.03), Vd_{ss} (2.28 ± 0.5 L) and Cl_{IPRL} (667 ± 74 ml/min/kg b.wt) were determined with k_{el} based on outflow concentrations (Table 2). Cl_{IPRL} was divided by

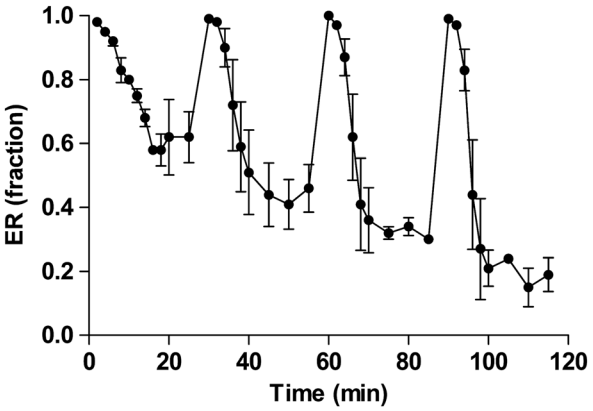

Figure 4. Hepatic extraction ratio of verapamil during IPRL experiments (ER_{IPRL}), points represent mean values (n = 3) ± SEM. ER_{IPRL} was calculated with Equation (10)

fu_{IPRL} (0.50 ± 0.04) to obtain a mean $Cl_{int,IPRL,u}$ of 1335 ml/min/kg b.wt.

Metabolic clearance of verapamil by suspended rat hepatocytes

Michaelis-Menten curves for verapamil metabolism were generated in freshly isolated and cryopreserved suspended rat hepatocytes (Figure 5), yielding statistically significantly different K_m values (4.6 ± 0.4 and 2.7 ± 0.3 μM; $p < 0.001$) and similar V_{max} values (561 ± 23 and 536 ± 34 pmol/min/million cells; $p > 0.05$) (Table 3). The latter is clearly illustrated in Figure 5. With an *F*-test it was confirmed that there was a statistically significant difference between the freshly isolated and cryopreserved suspended rat hepatocytes ($p < 0.01$). Unbound intrinsic clearance values were calculated. The $Cl_{int,hep,u}$ values were 142 and 250 μl/min/million cells for freshly isolated and cryopreserved suspended rat hepatocytes, respectively ($p < 0.05$). Although the V_{max} values were not significantly different, intrinsic clearance predictions still varied due to the significant difference in the mean K_m and fu_{hep} values. The $Cl_{int,hep,u}$ values were scaled-up using HPGL (163 million cells/g liver) and g liver/kg b.wt (35 g liver/kg b.wt, determined from IPRL experiments) to produce $Cl_{int,\ organ}$ values of 23 and 41 ml/min/g liver, respectively (Table 4) [35]. Subsequently, the well-stirred model was applied to convert the organ *Cl* values to an *in vivo Cl* (55 and 61 ml/min/kg b.wt). The resulting values were compared with rat liver microsomes,

DOI: 10.1002/bdd

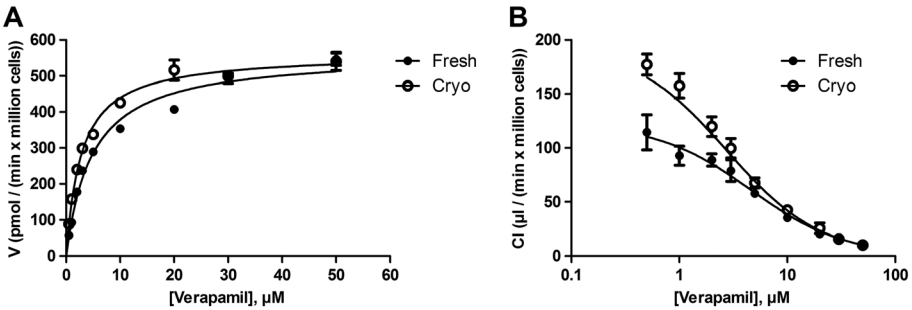

Figure 5. (A) Michaelis-Menten plots of verapamil metabolism by freshly isolated (closed circles) and cryopreserved (open circles) suspended rat hepatocytes (F-test p value < 0.01). Points represent mean values ± SEM of triplicate incubations with three batches (fresh) and three pools of three batches (cryopreserved) suspended rat hepatocytes ($n = 9$). (B) Verapamil clearance in suspended rat hepatocytes as a function of concentration. Points represent mean values ± SD

Table 3. Michaelis-Menten parameters (K_m, $K_m \times fu$, V_{max}) for the metabolism of verapamil in different preclinical model systems along with calculated total and unbound intrinsic clearance values (Cl_{int} and Cl_{int}/fu)

	Model system		
Parameter	Fresh SRH	Cryo SRH	RLM
K_m (µM)	4.6 ± 0.4	2.7 ± 0.3	4.1 ± 0.3
$K_m \times fu$ (µM)	3.9 ± 0.3	2.1 ± 0.2	2.8 ± 0.2
$Kp_{u,u}$ (ratio of unbound intra- to extracellular concentration)	**0.71 ± 0.08**	**1.31 ± 0.18**	-
V_{max} (pmol/min/million cells[a] or mg protein[b])	561 ± 23[a]	536 ± 34[a]	1889 ± 123[b]
Cl_{int} (µl/min/million cells[a] or mg protein[b])	123 ± 11[a]	195 ± 26[a]	457 ± 48[b]
Cl_{int}/fu (µl/min/million cells[a] or mg protein[b])	142 ± 18[a]	250 ± 35[a]	673 ± 73[b]
$Cl_{int}/(fu \times Kp_{u,u})$ (µl/min/million cells)	200 ± 33	191 ± 37	252 ± 27[c]

[a]pmol/min/million cells
[b]pmol/min/mg protein
[c]$Cl_{int,mic,u}$ was recalculated to match the unit of µl/min/million cells, using the conventional MPPMC from Table 5, no $Kp_{u,u}$-correction was applied here. Values are means ± SD (n = at least 3).

Table 4. Mean unbound clearance values at various levels, based on the preclinical systems used

Level	Clearance	RLM	Fresh SRH	Cryo SRH	IPRL	*In vivo*
Intracellular	$Cl_{int,intracellular}$ (µl/min/million cells)	**252 ± 27**	200 ± 33	191 ± 37	-	-
Cellular	$Cl_{int,cellular}$ (µl/min/million cells)	179 ± 27[a]	**142 ± 18**	**250 ± 35**	-	-
Organ	$Cl_{int,organ}$ (ml/min/g liver)	29 ± 5	23 ± 3	41 ± 6	**38 ± 4**	-
In vivo	$Cl_{in\ vivo}$ (ml/min/kg b.wt)	58	55	61	60	**53 ± 7**

Rat liver microsome data were scaled from mg protein to million cells, using conventional values for MPPGL (61 mg protein/g liver) and HPGL (163 million cells/g liver) [35]. $Cl_{int,intracellular}$ as determined with fresh and cryo SRH were calculated with Equation (7).
[a]$Cl_{int,cellular}$ as determined with rat liver microsomes, was calculated by multiplying $Cl_{int,mic,u}$ with the $Kp_{u,u}$ determined with freshly-isolated SRH. Predictions were recalculated to the subsequent level with the use of conventional scaling factors. Predicted hepatic $Cl_{int,organ}$ values were converted to an *in vivo* clearance by applying the well-stirred model ($Q_{H,B}$ = 70 ml/min/kg b.wt) [30]. Values are means ± SD (n = at least 3). Experimentally determined values are depicted in bold

IPRL and *in vivo* data in Table 4. For comparison with rat liver microsome data, the measured $Cl_{int,hep,u}$ values were also corrected for $Kp_{u,u}$ according to Equation (7), yielding $Cl_{int,hep,intracellular}$ values of 200 and 191 µl/min/million cells for fresh and cryopreserved hepatocytes, respectively, which were not statistically significantly different ($p > 0.05$).

Metabolic clearance of verapamil by rat liver microsomes

Verapamil metabolic disappearance rates during rat liver microsome incubations with increasing concentrations of verapamil are shown in Figure 6. The K_m and V_{max} were 4.1 ± 0.3 µM and

DOI: 10.1002/bdd

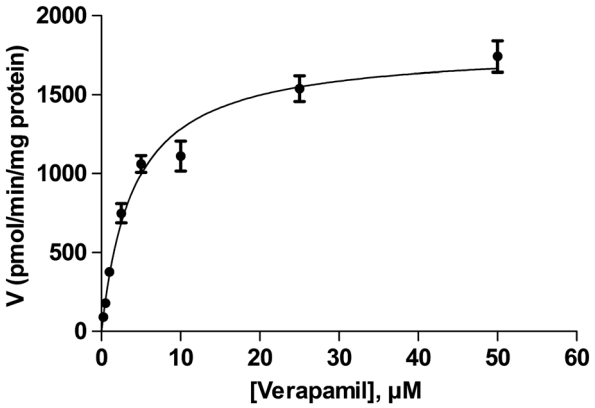

Figure 6. Michaelis-Menten plot of verapamil metabolism by rat liver microsomes. Points represent mean values ± SEM of two independent experiments with triplicate incubations ($n = 6$). rat liver microsomes pools were prepared from three rat livers

1889 ± 123 pmol/min/mg protein, respectively. All parameters are summarized in Table 3. K_m determined with rat liver microsomes, or Km_{mic} was corrected for binding as described with Equation (5). The $Km_{mic,u}$ corresponds to Km_{enzyme} (Figure 1) and was used to calculate $Kp_{u,u}$ according to Equation (6). $Cl_{int,mic,u}$ was calculated according to Equation (3) and amounted to 673 µl/min/mg protein or 252 µl/min/million cells if scaled by MPPMC (0.37 mg/million cells, calculated from MPPGL (61 mg microsomal protein/g liver) and HPGL (163 million cells/g liver) [35]. $Cl_{int,mic,u}$ was scaled up to the cellular level by multiplying it with the average $Kp_{u,u}$ (0.71) based on freshly isolated suspended rat hepatocytes, to acquire a cellular Cl_{int} of 179 µl/min/million cells (Table 4).

Calculation and application of $Kp_{u,u}$

The $Km_{hep,u,ex}$ values (3.9 ± 0.25 µM and 2.1 ± 0.22 µM for freshly isolated and cryopreserved cells, respectively) were calculated according to Equation (4) and divided by Km_{enzyme} (2.8 ± 0.2 µM) to determine $Kp_{u,u}$ according to Equation (6). The $Kp_{u,u}$ values were 0.71 ± 0.08 and 1.31 ± 0.18 for fresh and cryopreserved suspended rat hepatocytes, respectively. Hepatocyte-derived $Cl_{int,hep,intracellular}$ was calculated with Equation (7) and compared with $Cl_{int,mic,u}$. The $Cl_{int,hep,intracellular}$ values were 200 and 191 µl/min/million cells for fresh and cryopreserved suspended rat hepatocytes, respectively (Table 4). These values were used for direct comparison between rat liver microsomes and suspended rat hepatocytes and to determine activity-based scaling factors with Equations (8), (12), (13) and (16). The resulting scaling factors for MPPMC, MPPGL, HPGL and $Q_{H,B}$ are shown in Table 5.

In vivo predictions

In order to visually assess the accuracy of predicted Cl_{int} values, simulations were performed with predicted *in vitro* and *ex vivo* clearance values (Figure 7). Only previously reported values for MPPMC, MPPGL, HPGL and $Q_{H,B}$ were used for this comparison. To evaluate the different graphs compared with the observed PK-profile, R^2 and the residual sum of squares (RSS) were determined and compared in Table 6. The accuracy of predictions was ranked: freshly isolated SRH > RLM > IPRL > cryopreserved SRH, with

Table 5. Activity-based rat scaling factors for MPPMC, HPGL, MPPGL and $Q_{H,B}$ as calculated in the present study in comparison with 'conventional' rat scaling factors as reported previously

	Activity-based[a]			CYP450-content based
Rat scaling factors	Fresh SRH	Cryo SRH	IPRL	Conventional (rat)
MPPMC (mg protein/million cells)	0.30 ± 0.02	0.28 ± 0.03	/	0.37[b]
MPPGL (mg protein/g liver)	80 ± 15	43 ± 14	/	44.5[a] / 45[c] / 61[d]
HPGL (million cells/g liver)	269 ± 44	153 ± 27	/	120[c] / 163[d]
$Q_{H,B}$ (ml/min/kg b.wt)	/	/	61 ± 9	55.2[e] – 70[e]

Values are means ± SD.
[a]Determined in the present study.
[b]Calculated from the conventional MPPGL and HPGL stated by Smith *et al.*
[c]Reported by Barter *et al.* [49].
[d]Reported for the Wistar rat by Smith *et al.* [35].
[e][30,33].

DOI: 10.1002/bdd

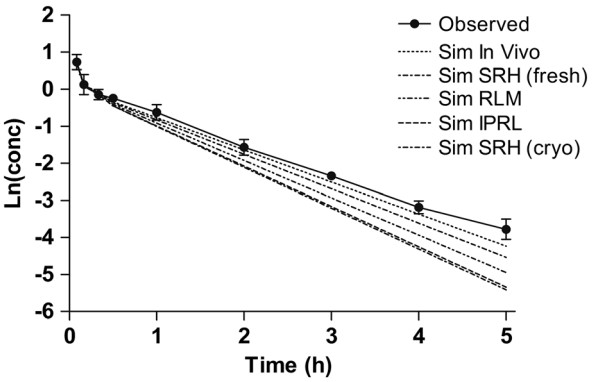

Figure 7. Ln(blood concentration, mg/l)-time curves, observed and predicted, while assuming a two-compartmental model, in Microsoft Excel 2010. For each model system, the elimination slope value (β) was obtained from predicted Cl_{int} values (Eq. (20)). The PK-profiles in the legend are ranked in the order in which the curves are plotted. This rank-order also reflects their predictive value when $Q_{H,B} = 70$ ml/min/kg b.wt.

Table 6. Accuracy of regression parameters (R^2 and RSS) between observed and predicted PK-profiles in Microsoft Excel 2010 (Figure 7)

Parameter	R^2	RSS
Combined *in vivo*	1.00	0.00
Sim *in vivo*	0.98	0.31
Sim SRH (fresh)	0.95	0.98
Sim RLM	0.87	2.50
Sim IPRL	0.76	4.72
Sim SRH (cryo)	0.74	5.21

Values were obtained *Cl* values scaled according to conventional scaling factor for MPPGL (61 mg protein/g liver) and HPGL (163 million cells/g liver) [35].

R^2 values of 0.95, 0.87, 0.76 and 0.74, respectively. By using $Cl_{in\ vivo}$ and $Cl_{int,IPRL,u}$ values in Equation (16), an activity-based value for $Q_{H,B}$ was calculated to be 60.9 ± 9.3 ml/min/kg b.wt (see Table 5). A value that is consistent with $Q_{H,B}$ values (55.2 and 70 ml/min/kg b.wt) reported and applied in the literature.

Discussion

Reliable drug clearance prediction with preclinical models for hepatic drug disposition, requires a complete understanding of all the limitations of these model systems in view of the systems' (in) ability to mimic the *in vivo* circumstances governing drug elimination. One approach to improve this understanding is the direct comparison of clearance values obtained with a model drug between the various model systems of increasing complexity, including *in vivo*. We have presently applied this concept with verapamil as a model drug, using rat liver microsomes (RLM), suspended rat hepatocytes (SRH; fresh/cryo) and the isolated perfused rat liver (IPRL) as model systems. Verapamil was chosen as a model drug because it is metabolically cleared solely via known CYP450 pathways, i.e. Cyp3a1/2 and Cyp1a2 in the rat liver. It reaches the intracellular compartment without the involvement of active uptake transport and is eliminated almost exclusively by the liver [19,20,36].

To compare the various *in vitro* models regarding their predictive accuracy of *in vivo* verapamil kinetics, the IPRL model serves as a benchmark to bridge the gap between *in vitro* and *in vivo*. $Cl_{int,IPRL}$ was determined based on the hepatic outflow concentrations. In this way, the equilibrium between liver and perfusate concentrations could be assumed as soon as the distribution phase was over, allowing a direct calculation of $Cl_{int,IPRL,u}$. The overestimation of the calculated $Cl_{int,in\ vivo,u}$ by the observed average $Cl_{int,IPRL,u}$ (Table 2), could be explained by oversimplification of the *in vivo* situation by the well-stirred model (Eq. (15)). Otherwise, variability in reported $Q_{H,B}$ values could lie at the basis of dissimilarities between *in vivo* and *ex vivo* Cl_{int} values. Therefore, $Q_{H,B}$ was calculated based on $Cl_{in\ vivo}$ and $Cl_{int,IPRL,u}$ which yielded a value of 61 ml/min/kg b.wt., a value which perfectly fits within the range of reported $Q_{H,B}$ values (55.2 and 70 ml/min/kg b.wt.) (Table 5). This calculated value did not differ significantly when calculated with other mathematical models such as the parallel tube and dispersion model (supplemental Table 5). Note that the hepatic extraction ratio (ER) during IPRL experiments with verapamil was not a constant and thus not used to calculate Cl_{IPRL}. While the initial drop in the extraction ratio was caused by verapamil distribution, the decrease in ER_{IPRL} after subsequent dosing (Figure 4) can likely be attributed to mechanism-based inhibition [36,26]. Verapamil and its primary metabolite nor-verapamil are known mechanism-based inhibitors. While the inhibitory effect of these

DOI: 10.1002/bdd

metabolites cannot be excluded, especially after subsequent dosing, it will be inherent to all clearance predictions with every preclinical model in this study [36,26].

As with IPRL, the disappearance rate of verapamil from the whole system in suspended rat hepatocytes was measured with reference to an (unbound) extracellular concentration (i.e. perfusate or incubation medium, respectively). This enabled a direct comparison between these systems without the use of mathematical models. [35]. Thus, the metabolism data obtained with suspended rat hepatocytes allow a comparison between rat liver microsomes and isolated perfused rat liver to determine the MPPMC and MPPGL values.

Comparison of verapamil metabolism kinetics between suspended rat hepatocytes and rat liver microsomes enabled us to propose a new method to calculate the intra- to extracellular unbound concentration ratio ($Kp_{u,u}$). This ratio has proven crucial for accurate IVIVE of clearance using rat liver microsomes as well as calculations regarding the intracellular unbound concentration [10]. In addition, it appeared that $Kp_{u,u}$ could enable more relevant scaling between microsomes and other liver models. It should be emphasized that our approach to derive $Kp_{u,u}$ relies on the ratio of unbound K_m (affinity) values only and not activity, implying that the accurately determined kinetics of verapamil metabolism are used as a tool to determine indirectly the free intra- to extracellular concentration ratio. Currently, no method is available to determine whether the compound-specific affinity (K_m) of P450 enzymes shifts when the cytosolic environment is replaced by a phosphate buffer (pH7.4). However, studies with compounds possessing low binding properties (tolbutamide, caffeine) show there is little difference in K_m values determined with suspended rat hepatocytes and rat liver microsomes [25,37]. Thus, we do not expect the intracellular $Km_{hep,u,in}$ to differ greatly from $Km_{mic,u}$.

Table 4 illustrates that the discrepancy in observed 'cellular' *Cl* values (expressed as µl/min/million cells) between freshly isolated and cryopreserved cells disappears when $Cl_{int,u}$ values determined with hepatocytes are corrected for $Kp_{u,u}$, resulting in 'intracellular' hepatocyte-based clearance values. However, the discrepancy between the microsomal clearance (i.e. 252 µl/min/million cells) obtained after conversion with the 'conventional' scaling factor for MPPMC of 0.37 mg/million cells and the intracellular hepatocyte-based *Cl* values is not resolved in the present study (Table 4). The conventional scaling factor is indeed higher than the average activity-based scaling factor derived here (0.29 ± 0.02 mg microsomal protein per million cells). Based on the IPRL calibration mentioned above, hepatocyte-based *Cl* values can be considered a reference in the comparison between IPRL and RLM. We therefore proposed a revised, activity-based scaling factor for rat liver microsomes-based clearance predictions (Eq. (8) and Table 5). The average MPPMC values calculated here (0.30 and 0.28 mg protein/million cells), corresponded very well to previously reported activity-based MPPMC values (0.3 mg protein/million cells) [1,25], but are significantly lower than the 'conventional' CYP450 content based MPPMC (0.37 mg protein/million cells). This modified value for MPPMC obviously propagates into the scaling from mg microsomal protein to g liver (MPPGL) (Eq. (13) and Table 5). [35]. The actual reason for lower activity-based scaling factor with rat liver microsomes (compared with CYP450-based scaling) will require further investigation. However, with respect to the functionality of P450 enzymes outside the cytosolic environment, Berezhkovskiy showed that a pH of 7.4 does not have a significant influence on P450 activity when compared with incubations performed at a pH of 7.0 [38]. In addition, when rat liver microsomes are incubated in isolated cytosol, changes in the unbound fractions due to the additional presence of protein would have to be determined experimentally. Another factor potentially complicating between-model comparison of CYP450-activity could be a differential contribution of positive cooperation between P450 enzymes. Thus apparently changing the amount of P450 enzyme needed to attain the same amount of drug turnover. This concept may also complicate the use of a universal scaling factor regarding MPPMC, since cooperativity could be compound-dependent [39].

The previously mentioned concordance in determined $Cl_{int,hep,intracellular}$ values between freshly isolated and cryopreserved hepatocytes (Table 4) ($p = 0.87$), indicates that the 'inherent' metabolic activity of hepatocytes is essentially unaffected

DOI: 10.1002/bdd

by cryopreservation. Nevertheless, the significant difference between the average $Kp_{u,u}$ values from freshly isolated and cryopreserved hepatocytes, resulting from the significantly different K_m values, causes the predicted clearance values to diverge. This indicates that the difference in the intracellular unbound disposition of verapamil between freshly isolated and cryopreserved hepatocytes can affect the prediction of $Cl_{in\ vivo}$. The latter is in line with the importance of drug transporters for clearance prediction [34,40]. Indeed, the involvement of a drug transporter could contribute further to the uncoupling of metabolic enzyme kinetics determined with rat liver microsomes and suspended rat hepatocytes. Therefore, even though there is no evidence that uptake transporters affect the intracellular verapamil disposition, the difference in activity-based HPGL values between freshly isolated and cryopreserved suspended rat hepatocytes (80 and 43 million cells/g liver) is attributed to $Kp_{u,u}$. Likewise, the difference between the conventional abundance based HPGL and activity-based HPGL determined here, is caused by the fact that $Kp_{u,u}$ is not included in the direct scaling with the conventional abundance based scaling factor. Due to the absence of uptake transporter effects, the actual estimates (0.71 ± 0.08 and 1.31 ± 0.18) obtained for $Kp_{u,u}$ in freshly isolated and cryopreserved cells deserve some additional reflection. Differences between the $Kp_{u,u}$ values from fresh and cryopreserved hepatocytes could be attributed either to changes in the membrane structure after consecutive freezing and thawing, the selection of a cellular subpopulation by the freeze/thaw process, the applied Percoll® gradient or disturbed mechanisms of pH homeostasis [41]. The existence of a pH gradient over the hepatocellular membrane could account for $Kp_{u,u}$ being more than 1 for a weak base. It is well known that the intracellular pH of hepatocytes is slightly more acidic (7.0) than the extracellular pH (7.4), which could cause lipophilic amines such as verapamil to concentrate in the intracellular compartment [42]. However, it was recently shown that during *in vitro* incubations with suspended rat hepatocytes, cells struggle to maintain an intracellular pH of 7.0 in large incubation volumes buffered at pH7.4 [38]. This may explain why the calculated $Kp_{u,u}$, for verapamil is not as high as would be expected by its ionization factor (2.447) at an external pH of 7.4. This ionization factor describes the ratio of the intracellular to extracellular concentration of the neutral drug, which was reported in the literature [11]. As a lipophilic amine, verapamil is subject to lysosomal sequestration [43,44], which undoubtedly influences $Kp_{u,u}$. Nevertheless, the obtained $Kp_{u,u}$ values are a result of all the underlying processes regarding intracellular binding and sequestration. Previous studies have illustrated that these processes are at least partly maintained in suspended hepatocytes [15]. Although the current approach for $Kp_{u,u}$ calculation is presently applied to a single model drug relying on metabolism only for its hepatic elimination, the promising potential of this method for determining $Kp_{u,u}$ is supported by the cross-system calibration concept applied here. Future experiments would have to indicate whether the current method to determine $Kp_{u,u}$ could be applied for other passively permeating as well as actively transported compounds. Active uptake processes would have to reach steady-state conditions with the extracellular compartment before $Kp_{u,u}$ could be calculated. While considering active uptake, $Kp_{u,u}$ will be concentration-dependent, making it more difficult to determine.

Another possible reason for the dissimilarity between the average $Kp_{u,u}$ values is the disputed absence or presence of canalicular efflux transporters in fresh suspended rat hepatocytes (P-gp, Mrp2, Bcrp, Bsep) [45,46]. The presence of P-gp mediated efflux could be better maintained in fresh versus cryopreserved suspended rat hepatocytes. If these transporters remain active at the plasma membrane, this could be a possible explanation for the lower average $Kp_{u,u}$ value of verapamil in fresh suspended rat hepatocytes [47].

When transporters are involved, more complex hepatocyte-based *in vitro* systems (i.e. sandwich-cultured hepatocytes; SCH) will have to be compared with the suspended hepatocyte method. Especially with respect to drug transporters located at the canalicular membrane. However, protein expression and enzyme activities are altered over culture time, which may contribute to significant dissimilarities in the calculated $Kp_{u,u}$ values between the different *in vitro* systems and *ex vivo*/*in vivo* [48]. The latter will most likely apply to compounds that rely on active transport processes to reach the intracellular compartment. Nonetheless,

DOI: 10.1002/bdd

applying the current approach to SCH data may reveal an activity-based scaling factor for sandwich-cultured hepatocytes.

The verapamil *in vivo* clearance is predicted with the use of the well-stirred model (Table 5). Whereas there seemed only a slight difference in the predicted $Cl_{\text{in vivo}}$, this divergence already had a marked impact on the predicted PK profiles in Figure 7. In the end, this could be attributed to the use of conventional scaling factors, rather than activity-based scaling factors calculated in the current study. Thus, other compounds will have to be investigated to determine the same activity-based scaling factors and to determine the effect of $Kp_{u,u}$ on these factors.

Conclusion

In summary, this study has successfully cross-validated rat liver microsomes, suspended rat hepatocytes (both freshly isolated and cryopreserved) and the *ex vivo* IPRL system to predict the *in vivo* hepatic clearance of verapamil. This cross-validation resulted in activity-based scaling factors that could improve future clearance predictions. Also, a new method to determine the ratio of the unbound intracellular to unbound extracellular concentration ($Kp_{u,u}$) was proposed and applied to predict $Cl_{\text{int,hep,intracellular}}$ for a passively diffusing drug, verapamil. The use of simple parameters such as K_m and the fraction unbound make this an easily applicable method that can be implemented without the need for other labor-intensive procedures or expensive equipment for imaging. Further research will be needed with a larger set of compounds including compounds subject to active uptake/efflux transport to validate the proposed approach in this study.

Acknowledgements

The authors would like to thank Jos Van Houdt (Janssen, Beerse) for his help in determining the total microsomal CYP content.

The Agency for Innovation by Science and Technology [Agentschap voor innovatie door wetenschap en technologie (IWT), Flanders, Belgium], project number 111193 and the Laboratory for Drug Delivery and Disposition, KU Leuven Department of Pharmaceutical and Pharmacological Sciences supported the work.

Conflict of Interest

The authors have declared that there is no conflict of interest.

References

1. Houston JB. Utility of *in vitro* drug metabolism data in predicting *in vivo* metabolic clearance. *Biochem Pharmacol* 1994; **47**: 1469–1479.
2. Di L, Keefer C, Scott DO, *et al.* Mechanistic insights from comparing intrinsic clearance values between human liver microsomes and hepatocytes to guide drug design. *Eur J Med Chem* 2012; **57**: 441–448. doi:10.1016/j.ejmech.2012.06.043.
3. Soars MG, McGinnity DF, Grime K, *et al.* The pivotal role of hepatocytes in drug discovery. *Chem Biol Interact* 2007; **168**: 2–15. doi:10.1016/j.cbi.2006.11.002.
4. Lu C, Li P, Gallegos R, *et al.* Comparison of intrinsic clearance in liver microsomes and hepatocytes from rats and humans: evaluation of free fraction and uptake in hepatocytes. *Drug Metab Dispos* 2006; **34**: 1600–1605. doi:10.1124/dmd.106.010793.
5. Brown HS, Griffin M, Houston JB. Evaluation of cryopreserved human hepatocytes as an alternative *in vitro* system to microsomes for the prediction of metabolic clearance. *Drug Metab Dispos* 2007; **35**: 293–301. doi:10.1124/dmd.106.011569.
6. Hallifax D, Houston JB. Methodological uncertainty in quantitative prediction of human hepatic clearance from *in vitro* experimental systems. *Curr Drug Metab* 2009; **10**: 307–321.
7. Foster JA, Houston JB, Hallifax D. Comparison of intrinsic clearances in human liver microsomes and suspended hepatocytes from the same donor livers: clearance-dependent relationship and implications for prediction of *in vivo* clearance. *Xenobiotica* 2011; **41**: 124–136. doi:10.3109/00498254.2010.530700.
8. Parker AJ, Houston JB. Rate-limiting steps in hepatic drug clearance: comparison of hepatocellular uptake and metabolism with microsomal metabolism of saquinavir, nelfinavir, and ritonavir. *Drug Metab Dispos* 2008; **36**: 1375–1384. doi:10.1124/dmd.108.020917.
9. Obach RS. Prediction of human clearance of twenty-nine drugs from hepatic microsomal intrinsic clearance data: an examination of *in vitro* half-life approach and nonspecific binding to microsomes. *Drug Metab Dispos* 1999; **27**: 1350–1359.

10. Chu X, Korzekwa K, Elsby R, *et al.* Intracellular drug concentrations and transporters: measurement, modeling, and implications for the liver. *Clin Pharmacol Ther* 2013; **94**: 126–141. doi:10.1038/clpt.2013.78.
11. Berezhkovskiy LM. The corrected traditional equations for calculation of hepatic clearance that account for the difference in drug ionization in extracellular and intracellular tissue water and the corresponding corrected PBPK equation. *J Pharm Sci* 2011; **100**: 1167–1183.
12. Hagenbuch B. Drug uptake systems in liver and kidney: a historic perspective. *Clin Pharmacol Ther* 2010; **87**: 39–47. doi:10.1038/clpt.2009.235.
13. Niemi M, Pasanen MK, Neuvonen PJ. Organic anion transporting polypeptide 1B1: a genetically polymorphic transporter of major importance for hepatic drug uptake. *Pharmacol Rev* 2011; **63**: 157–181. doi:10.1124/pr.110.002857.
14. Köck K, Brouwer KLR. A perspective on efflux transport proteins in the liver. *Clin Pharmacol Ther* 2012; **92**: 599–612. doi:10.1038/clpt.2012.79.
15. Pfeifer ND, Harris KB, Yan GZ, Brouwer KL. Determination of intracellular unbound concentrations and subcellular localization of drugs in rat sandwich-cultured hepatocytes compared to liver tissue. *Drug Metab Dispos* 2013; **41**: 1949–1956.
16. Dollery CT. Intracellular drug concentrations. *Clin Pharmacol Ther* 2013; **93**: 263–266. doi:10.1038/clpt.2012.240.
17. Elliott WJ, Ram CVS. Calcium channel blockers. *J Clin Hypertens (Greenwich)* 2011; **13**: 687–689. doi:10.1111/j.1751-7176.2011.00513.x.
18. Klotz U. Antiarrhythmics: elimination and dosage considerations in hepatic impairment. *Clin Pharmacokinet* 2007; **46**: 985–996. doi:10.2165/00003088-200746120-00002.
19. Hanada K, Ikemi Y, Kukita K, *et al.* Stereoselective first-pass metabolism of verapamil in the small intestine and liver in rats. *Drug Metab Dispos* 2008; **36**: 2037–2042. doi:10.1124/dmd.107.020339.
20. Umehara K-I, Camenisch G. Novel *in vitro-in vivo* extrapolation (IVIVE) method to predict hepatic organ clearance in rat. *Pharm Res* 2012; **29**: 603–617.
21. Omura T, Sato R. The carbon monoxide-binding pigment of liver microsomes. I. Evidence for its hemoprotein nature. *J Biol Chem* 1964; **239**: 2370–2378.
22. Mazur CS, Kenneke JF, Goldsmith M-R, *et al.* Contrasting influence of NADPH and a NADPH-regenerating system on the metabolism of carbonyl-containing compounds in hepatic microsomes. *Drug Metab Dispos* 2009; **37**: 1801–1805. doi:10.1124/dmd.109.027615.
23. Annaert PP, Turncliff RZ, Booth CL, *et al.* P-glycoprotein-mediated *in vitro* biliary excretion in sandwich-cultured rat hepatocytes. *Drug Metab Dispos* 2001; **29**: 1277–1283.
24. Rostami-Hodjegan A, Tucker GT. Simulation and prediction of *in vivo* drug metabolism in human populations from *in vitro* data. *Nat Rev Drug Discov* 2007; **6**: 140–148. doi:10.1038/nrd2173.
25. Hayes KA, Brennan B, Chenery R, *et al. In vivo* disposition of caffeine predicted from hepatic microsomal and hepatocyte data. *Drug Metab Dispos* 1995; **23**: 349–353.
26. Wang J, Xia S, Xue W, *et al.* A semi-physiologically-based pharmacokinetic model characterizing mechanism-based auto-inhibition to predict stereoselective pharmacokinetics of verapamil and its metabolite norverapamil in human. *Eur J Pharm* 2013; **50**: 290–302. doi:10.1016/j.ejps.2013.07.012.
27. Rosenbaum SE. Basic Pharmacokinetics and Pharmacodynamics: An Integrated Textbook and Computer Simulations (1st edn). John Wiley & Sons, Inc: Hoboken, NJ, 2011.
28. Yang J, Jamei M, Yeo KR, *et al.* Misuse of the well-stirred model of hepatic drug clearance. *Drug Metab Dispos* 2007; **35**: 501–502. doi:10.1124/dmd.106.013359.
29. Ito K, Houston JB. Comparison of the use of liver models for predicting drug clearance using *in vitro* kinetic data from hepatic microsomes and isolated hepatocytes. *Pharm Res* 2004; **21**: 785–792.
30. Obach RS. Predicting clearance in humans from *in vitro* data. *Curr Top Med Chem* 2011; **11**: 334–339.
31. Fagerholm U. Presentation of a modified dispersion model (MDM) for hepatic drug extraction and a new methodology for the prediction of the rate-limiting step in hepatic metabolic clearance. *Xenobiotica* 2009; **39**: 57–71. doi:10.1080/00498250802562652.
32. Pollack GM, Brouwer KL, Demby KB, *et al.* Determination of hepatic blood flow in the rat using sequential infusions of indocyanine green or galactose. *Drug Metab Dispos* 1990; **18**: 197–202.
33. Davies B, Morris T. Physiological parameters in laboratory animals and humans. *Pharm Res* 1993; **10**: 1093–1095.
34. Di L, Feng B, Goosen TC, *et al.* A perspective on the prediction of drug pharmacokinetics and disposition in drug research and development. *Drug Metab Dispos* 2013; **41**: 1975–1993. doi:10.1124/dmd.113.054031.
35. Smith R, Jones RDO, Ballard PG, *et al.* Determination of microsome and hepatocyte scaling factors for *in vitro/in vivo* extrapolation in the rat and dog. *Xenobiotica* 2008; **38**: 1386–1398. doi:10.1080/00498250802491662.
36. Yin J, Meng Q, Dong X. Auto-inhibition of verapamil metabolism in rat hepatocytes of gel entrapment culture. *Biomed Pharmacother* 2011; **65**: 328–333. doi:10.1016/j.biopha.2011.04.011.
37. Ashforth EI, Carlile DJ, Chenery R, *et al.* Prediction of *in vivo* disposition from *in vitro* systems: clearance of phenytoin and tolbutamide using rat hepatic microsomal and hepatocyte data. *J Pharmacol Exp Ther* 1995; **274**: 761–766.
38. Berezhkovskiy LM, Wong S, Halladay JS. On the maintenance of hepatocyte intracellular pH7.0 in

the *in-vitro* metabolic stability assay. *J Pharmacokinet Pharmacodyn* 2013; **40**: 683–689. doi:10.1007/s10928-013-9339-8.
39. Denisov IG, Frank DJ, Sligar SG. Cooperative properties of cytochromes P450. *Pharmacol Ther* 2009; **124**: 151–167. doi:10.1016/j.pharmthera.2009.05.011.
40. Li R, Barton HA, Varma MV. Prediction of pharmacokinetics and drug–drug interactions when hepatic transporters are involved. *Clin Pharmacokinet* 2014; **53**: 659–678. doi:10.1007/s40262-014-0156-z.
41. De Loecker R, Fuller BJ, Gruwez J, *et al.* The effects of cryopreservation on membrane integrity, membrane transport, and protein synthesis in rat hepatocytes. *Cryobiology* 1990; **27**: 143–152.
42. Pollock AS. Intracellular pH of hepatocytes in primary monolayer culture. *Am J Physiol* 1984; **246**: 738–744.
43. Kaufmann AM, Krise JP. Lysosomal sequestration of amine-containing drugs: analysis and therapeutic implications. *J Pharm Sci* 2007; **96**: 729–746. doi:10.1002/jps.20792.
44. Kazmi F, Hensley T, Pope C, *et al.* Lysosomal sequestration (trapping) of lipophilic amine (cationic amphiphilic) drugs in immortalized human hepatocytes (Fa2N-4 cells). *Drug Metab Dispos* 2013; **41**: 897–905. doi:10.1124/dmd.112.050054.
45. Lundquist P, Englund G, Skogastierna C, *et al.* Functional ATP-binding cassette drug efflux transporters in isolated human and rat hepatocytes significantly affect assessment of drug disposition. *Drug Metab Dispos* 2014; **42**: 448–458. doi:10.1124/dmd.113.054528.
46. Bow DAJ, Perry JL, Miller DS, *et al.* Localization of P-gp (Abcb1) and Mrp2 (Abcc2) in freshly isolated rat hepatocytes. *Drug Metab Dispos* 2008; **36**: 198–202. doi:10.1124/dmd.107.018200.
47. Döppenschmitt S, Spahn-Langguth H, Regårdh CG, *et al.* Role of P-glycoprotein-mediated secretion in absorptive drug permeability: an approach using passive membrane permeability and affinity to P-glycoprotein. *J Pharm Sci* 1999; **88**: 1067–1072.
48. De Bruyn T, Chatterjee S, Fattah S, *et al.* Sandwich-cultured hepatocytes: utility for *in vitro* exploration of hepatobiliary drug disposition and drug-induced hepatotoxicity. *Expert Opin Drug Metab Toxicol* 2013; **9**: 589–616. doi:10.1517/17425255.2013.773973.
49. Barter ZE, Bayliss MK, Beaune PH, *et al.* Scaling factors for the extrapolation of *in vivo* metabolic drug clearance from *in vitro* data: reaching a consensus on values of human microsomal protein and hepatocellularity per gram of liver. *Curr Drug Metab* 2007; **8**: 33–45.